Dexmedetomidine alleviates anxiety-like behavior in mice following peripheral nerve injury by reducing the hyperactivity of glutamatergic neurons in the anterior cingulate cortex

Wei Gao
The First Affiliated Hospital of USTC: Anhui Provincial Hospital
Dan-dan Long
Anhui Provincial Hospital
Ting-ting Pan
The First Affiliated Hospital of USTC: Anhui Provincial Hospital
Rui Hu
USTC: University of Science and Technology of China
Dan-yang Chen
USTC: University of Science and Technology of China
Yu Mao
USTC: University of Science and Technology of China
Xiao-qing Chai
The First Affiliated Hospital of USTC: Anhui Provincial Hospital
Yan Jin
USTC: University of Science and Technology of China
Zhi Zhang
The First Affiliated Hospital of USTC: Anhui Provincial Hospital
Di Wang (di.wang@ustc.edu.cn)
University of Science and Technology of China https://orcid.org/0000-0002-1380-568X

Research Article

Keywords: dexmedetomidine, anxiolytic, anxiety, pain, anterior cingulate cortex, glutamatergic neurons.

Posted Date: September 21st, 2022

DOI: https://doi.org/10.21203/rs.3.rs-1950091/v1

Abstract

Background: Treatment of chronic pain is challenged by concurrent anxiety symptoms. Dexmedetomidine is known to produce sedation, analgesia, and anxiolysis. However, the neural mechanism of dexmedetomidine-elicited anxiolysis remains elusive. Here, we aimed to test the hypothesis that the anterior cingulate cortex might be involved in dexmedetomidine-induced anxiolysis in pain.

Methods: A common peroneal nerve ligation mouse model was used to test the dexmedetomidine-induced analgesia and anxiolysis by assessing mechanical allodynia, open-field, light-dark transition, and acoustic startle reflex tests. *In vivo* calcium signal fiber photometry and *ex vivo*whole-cell patch-clamp recordings were used to measure the excitability of glutamatergic neurons in anterior cingulate cortex. Modulation of glutamatergic neurons was performed by chemogenetic inhibition or activation via viral injection.

Results: Compared with vehicle, dexmedetomidine (4 μg/kg) alleviated mechanical allodynia ($P < 0.001$) and anxiety-like behaviors ($P < 0.001$). The glutamatergic neurons' excitability after dexmedetomidine administration was lower than that of the vehicle group ($P = 0.001$). Anxiety-like behaviors were rescued by inhibiting glutamatergic neurons in the model mice. Nociception-related anxiety-like behavior was induced by activation of glutamatergic neurons, which was rescued by dexmedetomidine.

Conclusions: The reduction in glutamatergic neuronal activity in anterior cingulate cortex may be involved in dexmedetomidine-elicited anxiolysis in chronic pain.

1. Introduction

Chronic pain remains a global medical problem, which commonly leads to concomitant mood disorders, including anxiety[1–3]. Chronic pain frequently elicits anxiety, which further worsens the pain[4]. The cycle of exacerbating pain and anxiety remains challenging to treat clinically. Traditional analgesic medications have limited effects on concurrent psychiatric symptoms, and existing antidepressants may not be promising candidates for the treatment of concomitant anxiety in chronic pain[5]. Thus, it is essential to seek new drugs to control comorbid anxiety symptoms in pain condition.

Dexmedetomidine, that a selective α2-adrenoreceptor agonist, is used as a sedative in clinic. In addition to sedation, when given systemically or intrathecally for acute postsurgical pain control [6–8], dexmedetomidine has a short-term analgesic action. Prior studies have suggested that the antinociceptive response is mainly mediated in the spinal cord via the facilitation of inhibitory synaptic transmission in the dorsal horn [9–13]. Furthermore, dexmedetomidine is useful to reduce anxiety in the perioperative period [7, 14, 15]. However, a more in-depth understanding of the precise neural mechanism underlying the anxiolytic action of dexmedetomidine is lacking [16, 17].

Pain-related anxiety is likely mediated by multiple brain regions, such as the amygdala, anterior cingulate cortex (ACC), and medial prefrontal cortex. In particular, ACC is a critical area for the integration of

sensory perception and emotional responses in chronic pain [18–20]. MRI outcomes showed that ACC undergoes structural and functional plasticity during chronic pain in osteoarthritis [21, 22]. Animal studies have more precisely revealed that the hyperactivity of ACC associated with nociception-related anxiety-like behaviors, such as neuronal hyperexcitability and presynaptic long-term potentiation, is implicated in this process [23, 24]. Given α2-adrenoreceptor expression throughout the brain, it is unknown whether the ACC may be implicated in the anxiolytic effects of dexmedetomidine in pain condition.

Dexmedetomidine could be useful for perioperative anxiety control [7, 15] and has an additional benefit of reducing postsurgical pain [6, 7]. This makes dexmedetomidine an attractive candidate for patients suffering from concurrent anxiety symptoms in pain condition. Neuropathic pain represents a broad category of pain syndromes. We utilized common peroneal nerve ligation (CPNL), a well-established model to assess nociception-related anxiety-like behaviors [2, 3, 24]. Herein, we hypothesized that dexmedetomidine produces anxiolysis in mice following peripheral nerve injury and that the underlying mechanism may involve alterations in the neural activity of glutamatergic neurons in the ACC. To test our hypothesis, we employed a combination of behavioral tests, fiber photometry, chemogenetic manipulation, and electrophysiologic approaches.

2. Materials And Methods

2.1 Animals

C57BL/6J male mice weighing 20 ± 5 g were purchased from Jackson Laboratories at 8–12 weeks of age. All mice were housed at five mice per cage in a colony with access to food and water *ad libitum*. All mice were housed in a specific pathogen-free environment with controlled ambient temperature (22 ± 2°C) and humidity (50 ± 10%) under a 12 h light-dark cycle (lights on from 7:00 to 19:00). The sham and common peroneal nerve ligation mice were housed in separate cages. The mice were marked by the ear mark in the right ear with different numbers. The experimenter who performed the pain-like and anxiety-like behaviors was blinded to the groups of the mice. All the study details were approved by the Animal Care Committee of the University of Science and Technology of China (USTC). The experiments were carried out in line with ARRVIE guidelines and Ethics Guidelines of Animal Care and Use in USTC.

2.2 CPNL procedure

The left hindlimbs were subjected to a CPNL surgical procedure, as previously described[2, 3, 24]. Briefly, the mice were anesthetized by isoflurane (1%-3%) during the surgery. The common peroneal nerve was visible between the anterior and posterior groups of muscles, running almost transversely, was ligated with chromic gut sutures 5 – 0 slowly until twitching of the digits. The skin was then sutured and cleaned. The animals in the sham group underwent the same surgery, but the nerve was not ligated.

2.3 Mechanical allodynia test

Mice were placed in a Plexiglas box with a wire grid floor and allowed to habituate for at least 30 minutes each day at two days before testing. Mechanical sensitivity was assessed based on the responsiveness

of the left hind paw to the application of a set of von-Frey filaments in ascending order from 0.02 to 1.0 g to the point of bending.

2.4 Anxiety-like behaviors test

For all behavioral tests, mice were habituated approximately 2 hours before testing and with access to food and water *ad libitum*. Dim light (~ 20 lux) was used in the room to minimize the anxiety of the animals. The chamber was cleaned with 75% ethanol and clean water after each test to remove olfactory cues.

2.4.1 OF test

Mice were gently placed in the center of an open field (OF) apparatus that consisted of a square area (25 × 25 cm^2) and a marginal area (50 × 50 × 25 cm^3). The mice were allowed to freely explore their surroundings. The movement trajectories of mice were recorded by camera for 6 minutes. Time spent and distances in the central area and total distances traveled were calculated using EthoVision XT 14 software[1–3].

2.4.2 LDT test

The light-dark transition (LDT) was tested by an apparatus consisted of a cage with two sections (21×42×25 cm). One chamber was brightly illuminated by white diodes (390 lux), whereas the other chamber was dark (2 lux). Mice were placed into the dark side and allowed to move freely between the two chambers. The movement trajectories of mice were recorded by camera for 10 minutes. The number of entries into the bright chamber and the duration of time spent there as indices of bright-space anxiety were calculated using EthoVision XT 14 software [25, 26].

2.4.3 ASR test

After a 15 min period of acclimation to the testing room in a chamber, mice were placed in a sound-proof chamber for the acoustic startle reflex (ASR) test [27]. After a 15 min habituation period inside the startle chamber, mice received 30 startle trials (20-ms white noise stimuli with intensities of 80, 90 or 100 dB), each of the three white noise stimuli was applied 10 times in random order. The resulting startle reflexes of the mice in the startle chamber were recorded for 600 ms after acoustic stimuli onset. The acoustic startle reflex amplitude was defined as the largest peak-to-trough response that occurred within 200 ms after the onset of the startle stimulus was analyzed using TDT system 3 software. The acoustic startle reflex amplitude of each stimulus intensity was calculated as the mean amplitude of 30 startle trials.

2.5 Dexmedetomidine treatments

To determine the dose response to dexmedetomidine, mechanical allodynia (2, 4, or 8 μg/kg, i.p.) and anxiety-like behaviors (2, or 4 μg/kg, i.p.) were assessed after the single administration of different dosages of dexmedetomidine in both male and female mice subjected to CPNL procedure. The sedation assessments were performed 30 minutes after each drug administration. The sedation rating scale of

Chuck et al was used [28]. The ratings were as follows: 5-awake, active: engaged in locomotion, rearing, head movements or grooming; 4-awake, inactive: eyes fully open, head up, little to no locomotion, rearing or grooming, normal posture; 3-mild sedation: eyes partly closed, head somewhat down, impaired locomotion including abnormal posture, use only some limbs, dragging and stumbling; 2-moderate sedation: head mostly or completely down, eyes partly closed, flattened posture, no spontaneous mostly or completely down, eyes partly closed, flattened posture, no spontaneous movement; 1-heavy sedation: eyes mostly closed, loss of righting reflex; 0-asleep: eyes fully closed, body relaxed, asleep. For intra-ACC administration, dexmedetomidine (2 μM) diluted in standard artificial cerebrospinal fluid (ACSF, 300 nl) was unilaterally delivered into the right ACC, and ACSF (300 nl) was applied as a control.

2.6 Stereotaxic surgery

Mice were anesthetized with pentobarbital (20 mg/kg, i.p.) and fixed in a stereotactic frame (RWD, China). After the skull surface was exposed with a midline scalp incision, the ACC site was defined using the following coordinates: anterior posterior (AP) from bregma: 1 mm, medial lateral (ML) from the midline: 0.3 mm, dorsal ventral (DV) from the brain surface: -1.45 mm. A volume of 200 nl of virus was unilaterally injected into the right ACC through calibrated glass microelectrodes connected to an infusion pump (UMP3, WPI, US) at a rate of 30 nl/min. The pipette remained in the injection site for 10 minutes at the end of infusion to avoid virus overflow. And then a guide cannula (O.D.0.41 mm-27 G/M3.5, RWD, Shenzhen, China) was unilaterally implanted above ACC site (AP: 1 mm; ML: 0.3 mm; DV: -1.25 mm).Dexmedetomidine (2 μM) or standard ACSF was injected into the ACC for 1 minute (approximately 300 nl) through an injection cannula (O.D. 0.20 mm-30G/M3.5, RWD, Shenzhen, China) with a PE tube 30 minutes after clozapine-N-oxide administration in CaMKIIα-hM3Dq-treated mice.

2.7 Immunofluorescence

Mice were deeply anesthetized with pentobarbital sodium (i.p., 20 mg/kg) and then perfused with saline followed by 4% PFA on day-10 after CPNL surgery. The brains were removed and postfixed in 4% PFA in PBS at 4°C overnight and then incubated in 20% and 30% sucrose solution overnight for dehydration. Coronal slices (40 μm) were cut on a cryostat microtome system (CM1860, Leica). For immunofluorescence, the sections with ACC were incubated with blocking buffer (0.5% Triton X-100, 10% normal donkey serum in PBS) for 1 hour at room temperature, and then treated with primary antibodies, including anti-c-Fos (1:500, rabbit, Synaptic Systems), anti-glutamate (1:200, mouse, Sigma), and anti-glutamate (1:500, rabbit, Sigma) with 0.3% Triton X-100 and donkey serum at 4°C for overnight, followed by corresponding fluorophore-conjugated secondary antibodies (1:500, Invitrogen) for 2 hours at room temperature. Fluorescence signals were visualized using a Zeiss LSM880 microscope.

2.8 *In vivo* fiber-optic calcium recording

Mice were anesthetized with 5% (w/v, i.p.) chloral hydrate and fixed in a stereotactic frame (RWD, Shenzhen, China). AAV-CaMK -GCaMP6m-EGFP (BrainVTA, Wuhan, China) was injected into right ACC at a volume of 200 nl for induction of fluorescent calcium indicator expression. The fiber-optic cannula (Inper, Hangzhou, China) was implanted in 0.2 mm above the place and fixed on the skull by using dental

cement and glue for measurement of fluorescent signals. Fiber photometry was performed at least 3 weeks after the viral injection.

2.9 Chemogenetic manipulation

AAV-CaMKIIα-hM4Di-mCherry (AAV2/9, 4.61×10^{12} vg/ml, BrainVTA, China) or AAV-CaMKIIα-hM3Dq-EGFP (AAV2/9, 5.85×10^{12} vg/ml, BrainVTA, China) at a volume of 200 nl was unilaterally injected into the right ACC. Behavioral tests and electrophysiological recordings were performed at least 3 weeks after viral injection. Clozapine-N-oxide (CNO, MCE, USA) was dissolved in 0.9% saline (1 mg/ml) and injected (5 mg/kg, i.p.) 40 min before behavior tests.

2.10 Whole-cell patch-clamp recording

The acute brain slices preparation was the same as previous study[29]. An infrared (IR)-differential interference contrast (DIC) microscope (BX51WI, Olympus, Japan) equipped with fluorescent fittings was used to visualize neurons in ACC slices. mCherry-labeled neurons were identified under a microscope during whole-cell patch-clamp recording. Whole-cell patch-clamp recordings were performed using patch pipettes (5–8 MΩ) pulled from borosilicate glass capillaries (VitalSense Scientific Instruments Co., Ltd., Wuhan, China) with an outer diameter of 1.5 mm on a four-stage horizontal puller (P-1000, Sutter Instruments, USA). Dexmedetomidine (2 μM) was perfused into the slice chamber on the recording cell. During the recording, the current level was recorded before (3 min), during (6 min), and after (5 min) the application of dexmedetomidine. Yohimbine (1 μM) was added to the standard artificial cerebrospinal fluid, the slices were incubated in this drug solution for at least 10 min before the experiments, and the baseline current was recorded for at least 3 min before the application of dexmedetomidine. The signals were recorded by a patch-clamp amplifier (MultiClamp 700B Amplifier, Digidata 1440A analog-to-digital converter, USA) and pClamp 10.7 software (Axon Instruments/Molecular Devices, USA). All recordings were Bessel-filtered at 2.8 KHz and sampled at 10 kHz. Neurons with series resistance below 30 MΩ and changing < 20% throughout the recording were used for analysis. The signals were analyzed using Clampfit software version 10.7 (Molecular Devices, Sunnyvale, CA).

2.11 Statistical analysis

The parametric data are expressed as the mean ± SD, and nonparametric data are presented as the median (IQR). Histograms and QQ-plots were used to assess whether the data conformed to a normal distribution. If the distribution was normal, GraphPad Prism version 8.0 (CA, USA) was used for statistical analysis and graphing. The unpaired two-tailed Student’s t-test was used for comparisons between two groups. One-way analysis of variance (ANOVA) or two-way ANOVA followed by Bonferroni test was used for multiple comparisons. Otherwise, the nonnormally distributed data were analyzed by a Mann-Whitney test. Statistical significance was accepted at $p < 0.05$.

3. Results

3.1 *Systemic dexmedetomidine alleviates allodynia and anxiety-like behavior in mice following CPNL surgery.*

The CPNL procedure caused mechanical allodynia, which manifested as a reduction in PWT in the ipsilateral hindlimb paw, lasting over at least 14 days postsurgically (Figure-1A and 1B). Concomitant with allodynia, a combination of OF, LDT, and ASR tests on postsurgical day-10 revealed that mice subjected to CPNL procedure displayed anxiety-like behavior (Figure-1C-E).

Given dexmedetomidine has been reported to reverse allodynia at a low dose (3 μg/kg) in mice after peripheral nerve injury [12], we thus examined antinociceptive response of different dosages of systemic dexmedetomidine (2, 4 or 8 μg/kg) in our study (Figure-2A). Compared with saline control, we found that systemic dexmedetomidine dose-dependently elicited a reversal of mechanical allodynia in the male mice subjected to sham or CPNL procedure (sham, $F_{(3, 16)} = 2.763$, $P = 0.076$; ligation, $F_{(3, 16)} = 17.82$, $P < 0.001$, Figure-2B). Of note, the dosage of 8 μg/kg systemic dexmedetomidine produced mild to moderate sedation (Figure-2C), which made it difficult for the mice to finish the further behavioral tests. The analgesic duration of 4 μg/kg dexmedetomidine lasted approximately 2.5 hours ($F_{(6, 48)} = 41.06$, $P < 0.001$; Figure-2D). Only 2 and 4 μg/kg doses were used for further evaluating the effects of dexmedetomidine on anxiety-like behavior (Figure-2E-H). In ASR test, startle amplitude was significantly reduced after 4 μg/kg dexmedetomidine treatment ($F_{(2, 12)} = 10.91$, $P = 0.002$). In OF test, 4 μg/kg dexmedetomidine significantly increased the time in center ($F_{(2, 27)} = 7.277$, $P = 0.003$) and distances in center ($F_{(2, 27)} = 7.183$, $P = 0.003$); without any change in total distance ($F_{(2,27)} = 1.907$, $P = 0.168$). In LDT test, 4 μg/kg dexmedetomidine significantly increased time in light area ($F_{(2, 27)} = 12.04$, $P < 0.001$) and frequency to light area ($F_{(2, 27)} = 6.873$, $P = 0.004$). Similar to those findings in male mice, we found that dexmedetomidine produced a comparable antinociceptive and anxiolytic effects in female mice (those data not shown). Therefore, 4 μg/kg dexmedetomidine was selected for the following experiments.

Furthermore, we performed an *in vivo* experiment using yohimbine, that an antagonist of presynaptic α2-adrenoreceptor, to find if systemic yohimbine (5 μg/kg) could reverse the antinociceptive and anxiolytic effect of dexmedetomidine in mice subjected to CPNL procedure (Figure-3A). Compared with dexmedetomidine alone, treatment with dexmedetomidine plus yohimbine reduced ipsilateral hind-limb PWT (Figure-3B), and worsened the anxiety-like behavior in mice subjected to CPNL procedure (Figure-3C-E).

3.2 *Hyperactivity of glutamatergic neurons in ACC is implicated in the development of CPNL in mice.*

In order to seek the brain area which involved in the pharmacological action of dexmedetomidine against pain and comorbid anxiety, we initially conducted a staining for c-Fos protein on brain slices because c-Fos staining is often used as an indirect marker of neuronal activity. The immunofluorescence staining results showed an enhancement of c-Fos signal in multiple brain regions of the mice subjected to CPNL

procedure (Figure-4A-C). In particular, ACC has been proposed to be a target for treating pain and comorbid anxiety. Thus, we considered that ACC, with a distribution of α2-adrenoreceptor as reported previously [24], might be a site for the anxiolytic action of dexmedetomidine in pain condition. The immunofluorescence co-staining of c-Fos and glutamate further showed that most of c-Fos signal in ACC was primarily co-expressed within glutamatergic neurons (Figur-4D and 4E). Afterwards, to verify whether ACC is involved in dexmedetomidine-elicited anti-nociception and anxiolysis, we examined the direct impact of dexmedetomidine perfusion on whole-cell patch-clamp recordings of ACC glutamatergic neurons in acute brain slices *ex vivo*. Electrophysiological results showed that dexmedetomidine (2 μM) perfusion induced an outward current, suggesting hyperpolarization of glutamatergic neurons (Figure-4F). Additionally, the electrophysiological effect of dexmedetomidine on glutamatergic neurons *ex vivo* was blocked by additional perfusion of yohimbine (1 μM) [30] (Figure-4G).

3.3 *Inhibition of glutamatergic neurons in ACC rescues allodynia and anxiety-like behavior in mice following CPNL procedure.*

Given the increased excitability of ACC glutamatergic neurons, we further investigated whether conditional inhibition of glutamatergic neurons is able to reverse nociception-related anxiety-like behavior in the CPNL-treated mice. We utilized chemogenetic inhibition by locally microinjected AAV-CaMKIIα-hM4Di-mCherry into ACC of wild-type mice and intraperitoneal injection of CNO to selectively inhibit glutamatergic neurons (Figure-5A). We found that mCherry-labeled hM4Di was specifically expressed in glutamatergic neurons three weeks after the microinjection (Figure-5B). Whole-cell patch-clamp recordings were carried out to confirm the reduction in neuronal excitability of glutamatergic neurons after CNO perfusion (Figure-5C). In terms of mechanical allodynia, our findings showed that chemogenetic inhibition led to an attenuation of PWT reduction following CNO treatment ($F_{(8, 112)} = 12.45$, $P < 0.001$, Figure-5D). Similarly, OF test (time in center, $P = 0.005$; distances in center, $P = 0.013$; total distance, $P = 0.169$; Figure-5E), LDT test (time in light area, $P < 0.001$; frequencies to light area, $P = 0.042$; Figure-5F), and ASR test ($P = 0.005$, Figure-5G) showed that anxiety-like behaviors were reduced following the treatment with CNO in CPNL-treated mice that received AAV-CaMKIIα-hM4Di-mCherry.

3.4 *Systemic dexmedetomidine reduces hyperactivity of ACC glutamatergic neurons in CPNL-treated mice.*

To assess whether the calcium signal activity of ACC glutamatergic neurons was altered in response to stimulation by 0.07 g von-Frey filaments, *in vivo* fiber photometry recording was performed in wild-type mice that received viral injection of AAV-CaMKIIα-GCaMP6m-EGFP that enabled specific expression of the EGFP-labeled calcium indicator GCaMP6m under the control of the CaMKIIα-promoter (Figure-6A). The virus was locally injected into the right ACC, and the calcium indicator was expressed in glutamatergic neurons after three weeks (Figure-6B). Compared with baseline prior to surgery, freely moving mice displayed a substantial increase in calcium signal following stimulation by 0.07 g von-Frey filaments on the ipsilateral hind paw on postsurgical day-10. Additionally, we utilized fiber photometry to record *in vivo* calcium signals of ACC glutamatergic neurons in the CPNL-treated mice with dexmedetomidine

treatment. The *in vivo* calcium signals of glutamatergic neurons collected from freely moving mice were weakened by dexmedetomidine (Figure-6C and 6D). Electrophysiological results showed an increase in current-elicited action potentials and a decrease in rheobases recorded in visualized glutamatergic neurons in ACC from CPNL-treated mice compared with sham control mice (action potential firing rate: current×group interaction, $F_{(5, 220)} = 28.15$, $P < 0.001$; rheobases: 192.2 ± 46.2 pA vs. 97.4 ± 32.1 pA, $P < 0.001$, n = 23 cells from three mice for each group; Figure-6E and 6F). Following treatment with systemic dexmedetomidine, the electrophysiological results implied that the activity of ACC glutamatergic neurons in acute brain slices was reduced in dexmedetomidine-treated mice (action potential firing rate: current×group interaction, $F_{(5, 220)} = 2.862$, $P = 0.016$; rheobases: 107.5 ± 46.7 pA vs. 149.1 ± 37.4 pA, $P = 0.002$, n = 24 cells from three mice in the saline group and 22 cells from three mice in the dexmedetomidine group; Figure-6G and 6H).

3.5 *Activation of glutamatergic neurons is rescued by micro-injection of dexmedetomidine into ACC.*

To selectively enhance the activity of ACC glutamatergic neurons, we performed chemogenetic activation by using unilateral micro-injection of AAV-CaMKIIα-hM3Dq-EGFP into right ACC (Figure-7A). EGFP-labeled hM3Dq was specifically expressed in glutamatergic neurons three weeks after viral injection (Figure-7B and 7C). Those hM3Dq-treated mice developed allodynia and anxiety-like behavior in response to systemic CNO (Figure-7D-G). To examine whether dexmedetomidine (2 μM, 300 nl) exerted antinociceptive and anxiolytic actions via specific inhibition of ACC glutamatergic neurons, dexmedetomidine was locally delivered into the right ACC by an implanted guide cannula 40 min after systemic administration of CNO into the hM3Dq-treated mice (Figure-7H). Remarkably, local dexmedetomidine alleviated mechanical allodynia ($P < 0.001$, Figure-7I) in the hM3Dq-treated mice that received systemic CNO. In ASR test, startle amplitude was reduced ($P < 0.001$, Figure-7J). In OF test (Figure-7K), local dexmedetomidine into ACC of hM3Dq-treated mice increased the time in center ($P < 0.001$) and distances in center ($P = 0.029$) in response to CNO. In LDT test (Figure-7L), hM3Dq-treated mice with CNO administration spent more time in light area ($P = 0.008$) and have more frequencies to light area ($P = 0.029$) after local dexmedetomidine injection.

4. Discussion

Given that dexmedetomidine has both anxiolytic and analgesic properties, it may be useful to potentially extend the therapeutic utility in the management of anxiety symptoms in pain condition. Prior studies have suggested that dexmedetomidine produces analgesia probably through the activation of peripheral and spinal noradrenergic inhibitory systems, but the underlying mechanism of dexmedetomidine-elicited anxiolytic action is not yet clear [10–13, 16, 17]. The current study revealed that systemic dexmedetomidine at subanesthetic doses attenuated anxiety-like behaviors in mice after traumatic peripheral nerve injury. Our findings provided cellular evidence revealing that dexmedetomidine provided a reduction in the neuronal excitability of ACC glutamatergic neurons, which may be, at least in part, involved in dexmedetomidine-elicited anxiolysis in mice following traumatic peripheral nerve injury.

The noradrenergic system, driven by noradrenaline interacting with different adrenergic receptors distributed throughout the nervous system, is crucial for many physiological activities in the body [31, 32]. In particular, there is accumulating evidence that pain is one of the sensations regulated by the noradrenergic system, mostly through the involvement of α2-adrenoceptors [33, 34]. The spinal cord plays a crucial role in the transmission and modulation of painful information. It has been reported that spinal noxious sensory transmission can be modulated by descending inhibitory modulation and/or facilitatory modulation. It has been well-documented that noradrenergic descending pathways exert an inhibitory effect on nociceptive neurons within the dorsal horn of the spinal cord through the activation of α2-adrenoceptors [35]. This has been further functionally confirmed by the intrathecal administration of α2-adrenoceptors agonist. The intrathecal administration of dexmedetomidine (0.1-1.0 μg) [13] produced spinally-mediated analgesia owing to the direct activation of abundantly distributed α2-adrenoreceptors in the spinal cord. It has also been demonstrated that low-dose systemic dexmedetomidine (3 μg/kg) reverses mechanical allodynia in mice after peripheral nerve injury via an involvement of spinal α2-adrenoreceptors [12]. As the major producer of noradrenaline at the supraspinal level, locus coeruleus (LC) contributes to noradrenergic descending modulation of painful information in the spinal cord. In addition to acting at the spinal level, systemic dexmedetomidine (3 or 10 μg/kg) can facilitate spinal inhibitory synaptic responses to produce analgesia by activation of LC-spinal descending noradrenergic inhibitory pathway [10]. It has been reported that α2-adrenoreceptors are widely distributed throughout the supraspinal sites, and ACC receives abundant noradrenergic projections and contains corresponding receptors [36, 37]. The local noradrenergic system in ACC is thus considered a potential action site of systemic dexmedetomidine in our study. This is evidenced by our findings that systemic administration of dexmedetomidine reduced the hyperactivity of glutamatergic neurons in ACC. Apart from a well-known descending LC-spinal projection for nociception, the ascending pathway passing through the LC may be responsible for noradrenergic inputs to higher centers, such as ACC, for advanced processing of emotional information in pain condition. Unfortunately, there is no direct evidence in our study whether ACC glutamatergic neurons that receive LC noradrenergic inputs alters in response to dexmedetomidine.

Anxiety commonly occurs in chronic pain states, and the coexistence of these diseases worsens the outcomes of both disorders. This tends to create a cycle of pain and anxiety symptoms that is difficult to break, making the treatment of such patients challenging. For example, concomitant anxiety and/or depression is estimated to affect approximately one in three patients with osteoarthritis-related pain [38, 39]. Anxiety may result from chronic pain, but anxiety also predicts subsequent pain outcomes before or after surgical arthroplasty [40, 41]. In particular, great efforts have been made to explore the critical role of ACC in the relationship between chronic pain and comorbid anxiety. For example, the hyperactivity of ACC neurons and presynaptic long-term potentiation due to neural plasticity, mediate the interaction between anxiety and chronic pain [24, 42]. The available evidence supporting α2-adrenoceptor agonist-produced analgesia has mostly been obtained from animal models after peripheral nerve injury [10, 12, 43, 44]. However, it has also been shown that dexmedetomidine or clonidine has an antinociceptive effect in mice with post-incisional pain and inflammatory pain [45–49]. These findings may expand the potential use of α2-adrenoceptor agonists to multiple pain conditions, but further studies are still needed.

5. Conclusions

Our findings in the animal study indicate that the low dose of dexmedetomidine may produce anxiolysis in pain condition without excessive sedation. And the reduction in glutamatergic neuronal activity in ACC may be involved in dexmedetomidine-elicited anxiolysis in chronic pain.

Declarations

Ethics approval and consent to participate: All the study details have been approved by the Animal Care Committee of the University of Science and Technology of China (USTCACUC192301052).

Consent for publicaiton: Not applicable.

Competing interests: The authors declare that they have no competing interests.

Data available: The data that support the findings of this study are available from the corresponding author upon reasonable request.

Authors' contributions: W. GAO: Conceptualization, Data curation, and Writing-Original draft; D. LONG: Data curation and Methodology; T. PAN: Formal analysis; R. HU: Data curation and Methodology; D. CHEN: Methodology and Software; Y. MAO: Data curation and Methodology; Y. JIN: Methodology, Writing-Original draft and Visualization; X. CHAI: Supervision; Z. ZHANG: Supervision; D. WANG: Writing-Reviewing and Editing.

Acknowledgments: The authors very much appreciate the valuable and critical discussion with Dr. Xin Wei about study design.

Funding: This work was supported by the National Key Research and Development Program of China (2021ZD0203105), National Natural Science Foundation of China (grants 82171218), and Natural Science Foundation of Anhui Province (2008085QC114).

References

1. Jin Y, Meng Q, Mei L, Zhou W, Zhu X, Mao Y, Xie W, Zhang X, Luo MH, Tao W, et al. A somatosensory cortex input to the caudal dorsolateral striatum controls comorbid anxiety in persistent pain. Pain. 2020;161:416–28.
2. Yin JB, Liang SH, Li F, Zhao WJ, Bai Y, Sun Y, Wu ZY, Ding T, Sun Y, Liu HX, et al. dmPFC-vlPAG projection neurons contribute to pain threshold maintenance and antianxiety behaviors. J Clin Invest. 2020;130:6555–70.
3. Li XH, Matsuura T, Xue M, Chen QY, Liu RH, Lu JS, Shi W, Fan K, Zhou Z, Miao Z, et al. Oxytocin in the anterior cingulate cortex attenuates neuropathic pain and emotional anxiety by inhibiting presynaptic long-term potentiation. Cell Rep. 2021;36:109411.

4. Zhuo M. Neural Mechanisms Underlying Anxiety-Chronic Pain Interactions. Trends Neurosci. 2016;39:136–45.
5. Locher C, Koechlin H, Zion SR, Werner C, Pine DS, Kirsch I, Kessler RC, Kossowsky J. Efficacy and Safety of Selective Serotonin Reuptake Inhibitors, Serotonin-Norepinephrine Reuptake Inhibitors, and Placebo for Common Psychiatric Disorders Among Children and Adolescents: A Systematic Review and Meta-analysis. JAMA Psychiatry. 2017;74:1011–20.
6. Kaye AD, Chernobylsky DJ, Thakur P, Siddaiah H, Kaye RJ, Eng LK, Harbell MW, Lajaunie J, Cornett EM. Dexmedetomidine in Enhanced Recovery After Surgery (ERAS) Protocols for Postoperative Pain. Curr Pain Headache Rep. 2020;24:21.
7. Schmidt AP, Valinetti EA, Bandeira D, Bertacchi MF, Simoes CM, Auler JO Jr. Effects of preanesthetic administration of midazolam, clonidine, or dexmedetomidine on postoperative pain and anxiety in children. Paediatr Anaesth. 2007;17:667–74.
8. Paramasivan A, Lopez-Olivo MA, Foong TW, Tan YW, Yap APA. Intrathecal dexmedetomidine and postoperative pain: A systematic review and meta-analysis of randomized controlled trials. Eur J Pain. 2020;24:1215–27.
9. Guo TZ, Jiang JY, Buttermann AE, Maze M. Dexmedetomidine injection into the locus ceruleus produces antinociception. Anesthesiology. 1996;84:873–81.
10. Funai Y, Pickering AE, Uta D, Nishikawa K, Mori T, Asada A, Imoto K, Furue H. Systemic dexmedetomidine augments inhibitory synaptic transmission in the superficial dorsal horn through activation of descending noradrenergic control: an in vivo patch-clamp analysis of analgesic mechanisms. Pain. 2014;155:617–28.
11. Fairbanks CA, Kitto KF, Nguyen HO, Stone LS, Wilcox GL. Clonidine and dexmedetomidine produce antinociceptive synergy in mouse spinal cord. Anesthesiology. 2009;110:638–47.
12. Malmberg AB, Hedley LR, Jasper JR, Hunter JC, Basbaum AI. Contribution of alpha(2) receptor subtypes to nerve injury-induced pain and its regulation by dexmedetomidine. Br J Pharmacol. 2001;132:1827–36.
13. Kimura M, Saito S, Obata H. Dexmedetomidine decreases hyperalgesia in neuropathic pain by increasing acetylcholine in the spinal cord. Neurosci Lett. 2012;529:70–4.
14. Lee-Archer PF, von Ungern-Sternberg BS, Reade M, Betts M, Haenke D, Keys A, Rance T, Gibbons K, Long D. The effect of dexmedetomidine on postoperative behaviour change in children: a randomised controlled trial. Anaesthesia. 2020;75:1461–8.
15. Du Z, Zhang XY, Qu SQ, Song ZB, Wei SW, Xiang Z, Guo QL. The comparison of dexmedetomidine and midazolam premedication on postoperative anxiety in children for hernia repair surgery: A randomized controlled trial. Paediatr Anaesth. 2019;29:843–9.
16. Ji MH, Jia M, Zhang MQ, Liu WX, Xie ZC, Wang ZY, Yang JJ. Dexmedetomidine alleviates anxiety-like behaviors and cognitive impairments in a rat model of post-traumatic stress disorder. Prog Neuropsychopharmacol Biol Psychiatry. 2014;54:284–8.

17. Jang M, Jung T, Kim SH, Noh J. Sex differential effect of dexmedetomidine on fear memory extinction and anxiety behavior in adolescent rats. Neurosci Res. 2019;149:29–37.
18. Smith ML, Asada N, Malenka RC. Anterior cingulate inputs to nucleus accumbens control the social transfer of pain and analgesia. Science. 2021;371:153–9.
19. Meda KS, Patel T, Braz JM, Malik R, Turner ML, Seifikar H, Basbaum AI, Sohal VS. Microcircuit Mechanisms through which Mediodorsal Thalamic Input to Anterior Cingulate Cortex Exacerbates Pain-Related Aversion. Neuron. 2019;102:944–59 e943.
20. Barthas F, Sellmeijer J, Hugel S, Waltisperger E, Barrot M, Yalcin I. The anterior cingulate cortex is a critical hub for pain-induced depression. Biol Psychiatry. 2015;77:236–45.
21. Soni A, Wanigasekera V, Mezue M, Cooper C, Javaid MK, Price AJ, Tracey I. Central Sensitization in Knee Osteoarthritis: Relating Presurgical Brainstem Neuroimaging and PainDETECT-Based Patient Stratification to Arthroplasty Outcome. Arthritis Rheumatol. 2019;71:550–60.
22. Russell MD, Barrick TR, Howe FA, Sofat N. Reduced anterior cingulate grey matter volume in painful hand osteoarthritis. Rheumatol Int. 2018;38:1429–35.
23. Zhou H, Zhang Q, Martinez E, Dale J, Hu S, Zhang E, Liu K, Huang D, Yang G, Chen Z, Wang J. Ketamine reduces aversion in rodent pain models by suppressing hyperactivity of the anterior cingulate cortex. Nat Commun. 2018;9:3751.
24. Koga K, Descalzi G, Chen T, Ko HG, Lu J, Li S, Son J, Kim T, Kwak C, Huganir RL, et al. Coexistence of two forms of LTP in ACC provides a synaptic mechanism for the interactions between anxiety and chronic pain. Neuron. 2015;85:377–89.
25. Wang GQ, Cen C, Li C, Cao S, Wang N, Zhou Z, Liu XM, Xu Y, Tian NX, Zhang Y, et al. Deactivation of excitatory neurons in the prelimbic cortex via Cdk5 promotes pain sensation and anxiety. Nat Commun. 2015;6:7660.
26. Zhang YQ, Lin WP, Huang LP, Zhao B, Zhang CC, Yin DM. Dopamine D2 receptor regulates cortical synaptic pruning in rodents. Nat Commun. 2021;12:6444.
27. Guo W, Fan S, Xiao D, Dong H, Xu G, Wan Z, Ma Y, Wang Z, Xue T, Zhou Y, et al. A Brainstem reticulotegmental neural ensemble drives acoustic startle reflexes. Nat Commun. 2021;12:6403.
28. Chuck TL, McLaughlin PJ, Arizzi-LaFrance MN, Salamone JD, Correa M. Comparison between multiple behavioral effects of peripheral ethanol administration in rats: sedation, ataxia, and bradykinesia. Life Sci. 2006;79:154–61.
29. Zhu X, Zhou W, Jin Y, Tang H, Cao P, Mao Y, Xie W, Zhang X, Zhao F, Luo MH, et al. A Central Amygdala Input to the Parafascicular Nucleus Controls Comorbid Pain in Depression. Cell Rep. 2019;29:3847–58 e3845.
30. Nomura S, Tricoire L, Cohen I, Kuhn B, Lambolez B, Hepp R. Combined Optogenetic Approaches Reveal Quantitative Dynamics of Endogenous Noradrenergic Transmission in the Brain. iScience. 2020;23:101710.
31. Sternberg Z, Schaller B. Central Noradrenergic Agonists in the Treatment of Ischemic Stroke-an Overview. Transl Stroke Res. 2020;11:165–84.

32. Paredes-Rodriguez E, Vegas-Suarez S, Morera-Herreras T, De Deurwaerdere P, Miguelez C. The Noradrenergic System in Parkinson's Disease. Front Pharmacol. 2020;11:435.
33. Pertovaara A. The noradrenergic pain regulation system: a potential target for pain therapy. Eur J Pharmacol. 2013;716:2–7.
34. Llorca-Torralba M, Borges G, Neto F, Mico JA, Berrocoso E. Noradrenergic Locus Coeruleus pathways in pain modulation. Neuroscience. 2016;338:93–113.
35. Patel R, Qu C, Xie JY, Porreca F, Dickenson AH. Selective deficiencies in descending inhibitory modulation in neuropathic rats: implications for enhancing noradrenergic tone. Pain. 2018;159:1887–99.
36. Koga K, Yamada A, Song Q, Li XH, Chen QY, Liu RH, Ge J, Zhan C, Furue H, Zhuo M, Chen T. Ascending noradrenergic excitation from the locus coeruleus to the anterior cingulate cortex. Mol Brain. 2020;13:49.
37. Cordeiro Matos S, Zamfir M, Longo G, Ribeiro-da-Silva A, Seguela P. Noradrenergic fiber sprouting and altered transduction in neuropathic prefrontal cortex. Brain Struct Funct. 2018;223:1149–64.
38. Axford J, Butt A, Heron C, Hammond J, Morgan J, Alavi A, Bolton J, Bland M. Prevalence of anxiety and depression in osteoarthritis: use of the Hospital Anxiety and Depression Scale as a screening tool. Clin Rheumatol. 2010;29:1277–83.
39. Fonseca-Rodrigues D, Rodrigues A, Martins T, Pinto J, Amorim D, Almeida A, Pinto-Ribeiro F. Correlation between pain severity and levels of anxiety and depression in osteoarthritis patients: a systematic review and meta-analysis. Rheumatology (Oxford). 2021;61:53–75.
40. Wood TJ, Thornley P, Petruccelli D, Kabali C, Winemaker M, de Beer J. Preoperative Predictors of Pain Catastrophizing, Anxiety, and Depression in Patients Undergoing Total Joint Arthroplasty. J Arthroplasty. 2016;31:2750–6.
41. Hassett AL, Marshall E, Bailey AM, Moser S, Clauw DJ, Hooten WM, Urquhart A, Brummett CM. Changes in Anxiety and Depression Are Mediated by Changes in Pain Severity in Patients Undergoing Lower-Extremity Total Joint Arthroplasty. Reg Anesth Pain Med. 2018;43:14–8.
42. Sellmeijer J, Mathis V, Hugel S, Li XH, Song Q, Chen QY, Barthas F, Lutz PE, Karatas M, Luthi A, et al. Hyperactivity of Anterior Cingulate Cortex Areas 24a/24b Drives Chronic Pain-Induced Anxiodepressive-like Consequences. J Neurosci. 2018;38:3102–15.
43. Yang Y, Xia Z, Meng Q, Liu K, Xiao Y, Shi L. Dexmedetomidine relieves neuropathic pain by inhibiting hyperpolarization-activated cyclic nucleotide-gated currents in dorsal root ganglia neurons. NeuroReport. 2018;29:1001–6.
44. Bahari Z, Meftahi GH. Spinal alpha2 -adrenoceptors and neuropathic pain modulation; therapeutic target. Br J Pharmacol. 2019;176:2366–81.
45. Wilsey JT, Block JH. Sustained analgesic effect of clonidine co-polymer depot in a porcine incisional pain model. J Pain Res. 2018;11:693–701.
46. Yamanaka D, Kawano T, Nishigaki A, Aoyama B, Tateiwa H, Shigematsu-Locatelli M, Locatelli FM, Yokoyama M. The preventive effects of dexmedetomidine on endotoxin-induced exacerbated post-

incisional pain in rats. J Anesth. 2017;31:664–71.

47. Wang XT, Lian X, Xu YM, Suo ZW, Yang X, Hu XD. alpha(2) noradrenergic receptor suppressed CaMKII signaling in spinal dorsal horn of mice with inflammatory pain. Eur J Pharmacol. 2014;724:16–23.
48. Fan QQ, Li L, Wang WT, Yang X, Suo ZW, Hu XD. Activation of alpha2 adrenoceptors inhibited NMDA receptor-mediated nociceptive transmission in spinal dorsal horn of mice with inflammatory pain. Neuropharmacology. 2014;77:185–92.
49. Xu YM, Wang XT, Zhang ZY, Suo ZW, Yang X, Hu XD. Noradrenergic alpha2 receptor attenuated inflammatory pain through STEP61/ERK signalling. Eur J Pain. 2015;19:1298–307.

Figures

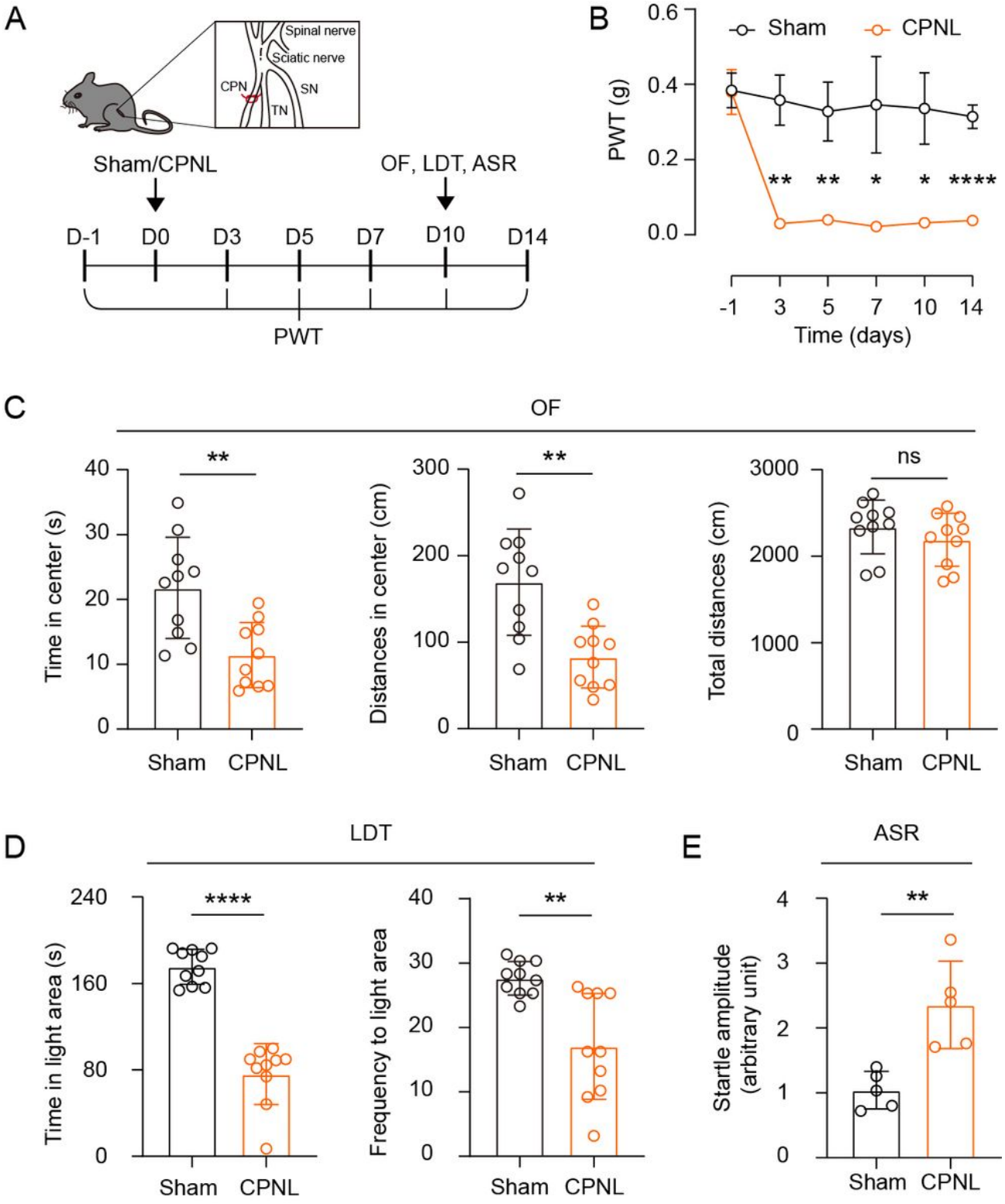

Figure 1

Changes in pain-related and anxiety-like behaviors after CPNL.

(A) Schematic of CPNL (left hind limb) and timeline of subsequent experiments. (B) Time course of CPNL-induced PWT. (n = 5 mice per group; time×group interaction, $F(5, 40) = 10.51$, $P < 0.001$). (C) Performance of mice treated with sham and CPNL on postsurgical day 10 in the OF test. (n = 10 mice per

group; time in center, t18 =3.531, *P* = 0.002; distances in center, t18 = 3.849, *P* = 0.001; total distance, t18 = 1.062, *P* = 0.302). (D) Performance of mice treated with sham and CPNL on postsurgical day 10 in the LDT test. (n = 10 mice per group; time in light area, t18 = 9.661, *P* < 0.001; frequency to light area, t18 = 3.878, *P* = 0.001). (E) Performance of mice treated with sham and CPNL on postsurgical day 10 in the ASR test. (n = 5 mice per group; startle amplitude, t8 = 3.998, *P* = 0.004). Compared with sham mice, * *P* < 0.05, ** *P* < 0.01, *** *P* < 0.001, **** *P* < 0.0001. Two-way repeated-measures (RM) ANOVA with Bonferroni post hoc analysis for (B), two-tailed unpaired Student's t test for (C, D and E). ANOVA, analysis of variance; ns, no significant difference; CPNL, common peroneal nerve ligation; PWT, paw withdrawal threshold; OFT, open field; LDT, light-dark transition; ASR, acoustic startle reflex.

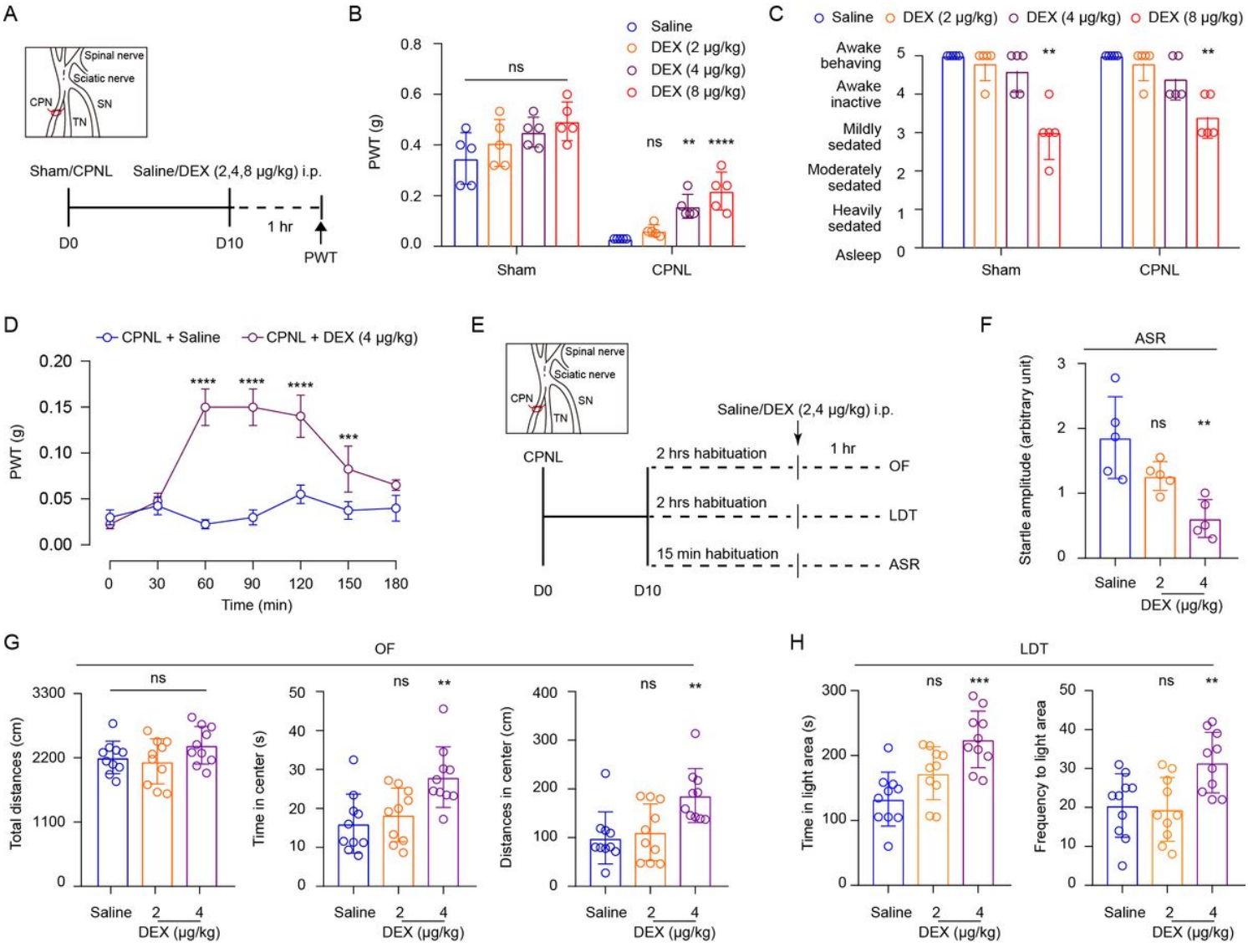

Figure 2

Dose-dependent effects of dexmedetomidine on analgesia and anxiety relief in CPNL mice.

(A) Timeline of the dose response to dexmedetomidineexperiments of PWT and sedation in sham and CPNL mice. Changes in PWT (B) and sedation score (C) of CPNL mice treated with DEX at various

concentrations. (n = 5 mice per group; sham, PWT: F(3, 16) = 2.763, $P = 0.076$, sedation score: H = 12.9, $P = 0.005$; CPNL, PWT: F(3, 16) = 17.82, $P < 0.001$, sedation score: H = 13.85, $P = 0.003$). (D) Time course of the effects of DEX (4 μg/kg) on PWT after CPNL. (n = 5 mice per group; time×group interaction, F(6, 48) = 41.06, $P < 0.001$). (E) Timeline of dose response to dexmedetomidine experiments on anxiety-like behavior test in CPNL mice. (F) Performance of CPNL mice treated with DEX in the ASR test (n = 5 mice per group; startle amplitude, F (2, 12) = 10.91, $P = 0.002$). (G) Performance of CPNL mice treated with DEX (2, or 4 μg/kg) in the OF test. (n = 10 mice per group; time in center, F (2, 27) = 7.277,$P = 0.003$, distances in center, F(2, 27) = 7.183, $P = 0.003$, total distance, F(2,27) = 1.907, $P = 0.168$). (H) Performance of CPNL mice treated with saline or DEX (2, or 4 μg/kg) in the LDT test (n = 10 mice per group; time in light area, F (2, 27) = 12.04, $P < 0.001$, frequency to light area, F (2, 27) = 6.873, $P = 0.004$). * $P < 0.05$, ** $P < 0.01$, *** $P < 0.001$, **** $P < 0.0001$, compared with Sham or CPNL + saline. Kruskal – Wallis test for (B-CPNL-PWT and C), one-way ANOVA with Bonferroni post hoc analysis for (B-sham-PWT, F, G and H), two-way repeated-measures (RM) ANOVA with Bonferroni post hoc analysis for (D). ANOVA, analysis of variance; ns, no significant difference; CPNL, common peroneal nerve ligation; PWT, paw withdrawal threshold; OF, open field; LDT, light-dark transition; ASR, acoustic startle reflex; DEX, dexmedetomidine.

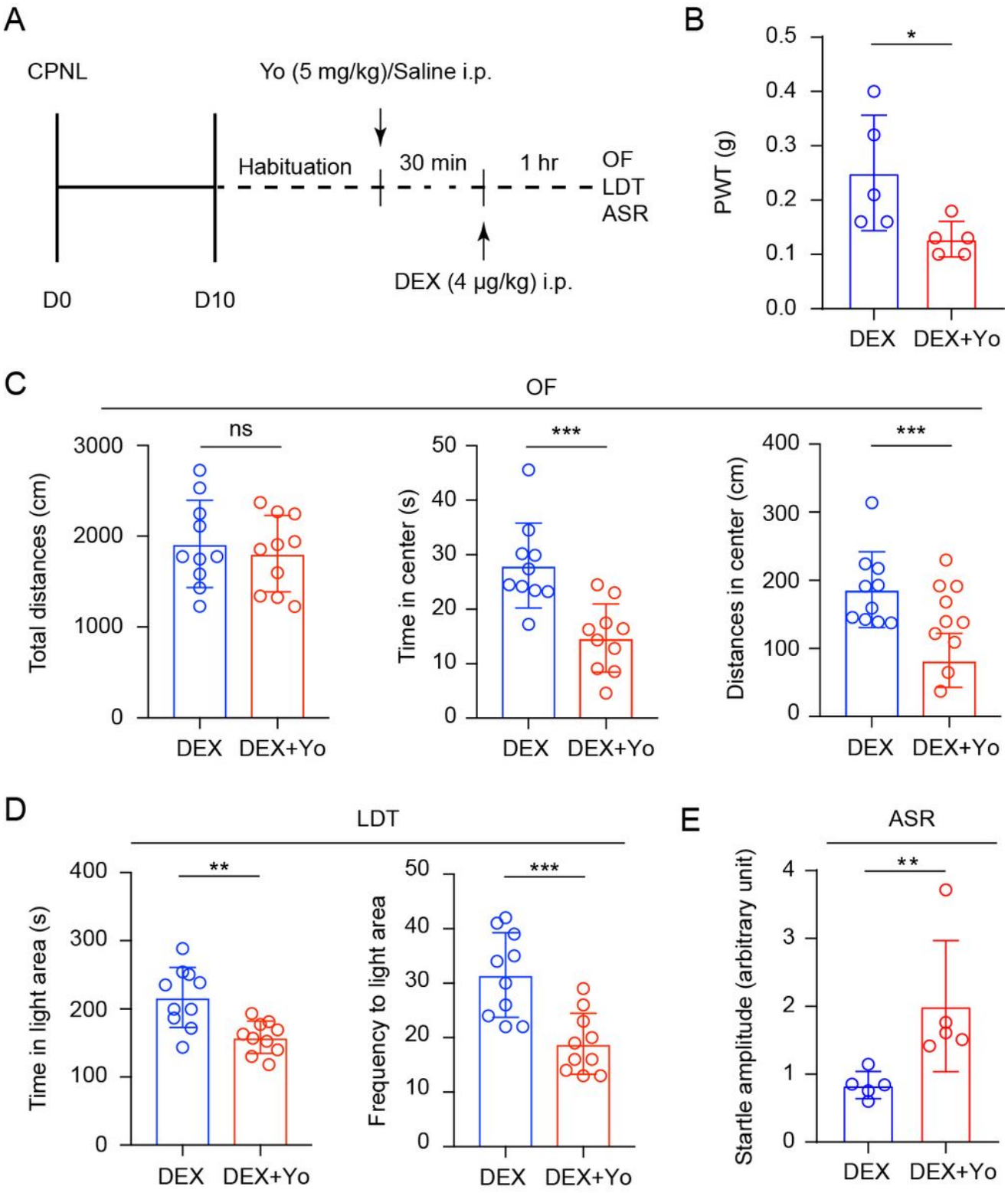

Figure 3

Yohimbine partly reversed the analgesic and antianxiety effects of DEX in CPNL mice.

(A) Timeline of the experiments on the effect of yohimbine on DEX-treated CPNL mice. (B) Changes in PWT of CPNL mice treated with saline or DEX after administration of yohimbine (n = 5 mice per group; PWT, t8 = 2.453, *P* = 0.040). (C) Performance of CPNL mice treated with saline or yohimbine after

administration of DEX in the OF test (n = 10 mice per group; time in center, t18 = 4.208,$P < 0.001$; distances in center, t18 = 4.823, $P < 0.001$; total distance, t18 = 0.5355, $P = 0.599$). (D) Performance of CPNL mice treated with saline or yohimbine after administration of DEX in the LDT test (n = 10 mice per group; time in light area, t18 = 3.71, $P = 0.002$; frequency to light area, t18 = 4.161, $P = 0.001$). (E) Performance of CPNL mice treated with saline or yohimbine after administration of DEX in the ASR test (n = 5 mice per group; startle amplitude, t8 = 2.637, $P = 0.030$). Compared with sham mice, $* P < 0.05$, $** P < 0.01$, $*** P < 0.001$, $**** P < 0.0001$. Two-tailed unpaired Student's t test for (B, C, D, and E). ns, no significant difference; CPNL, common peroneal nerve ligation; ACC, anterior cingulate cortex; GluACC neurons, glutamatergic neurons in the anterior cingulate cortex; DEX, dexmedetomidine; Yo, yohimbine; OFT, open field; LDT, light-dark transition; ASR, acoustic startle reflex.

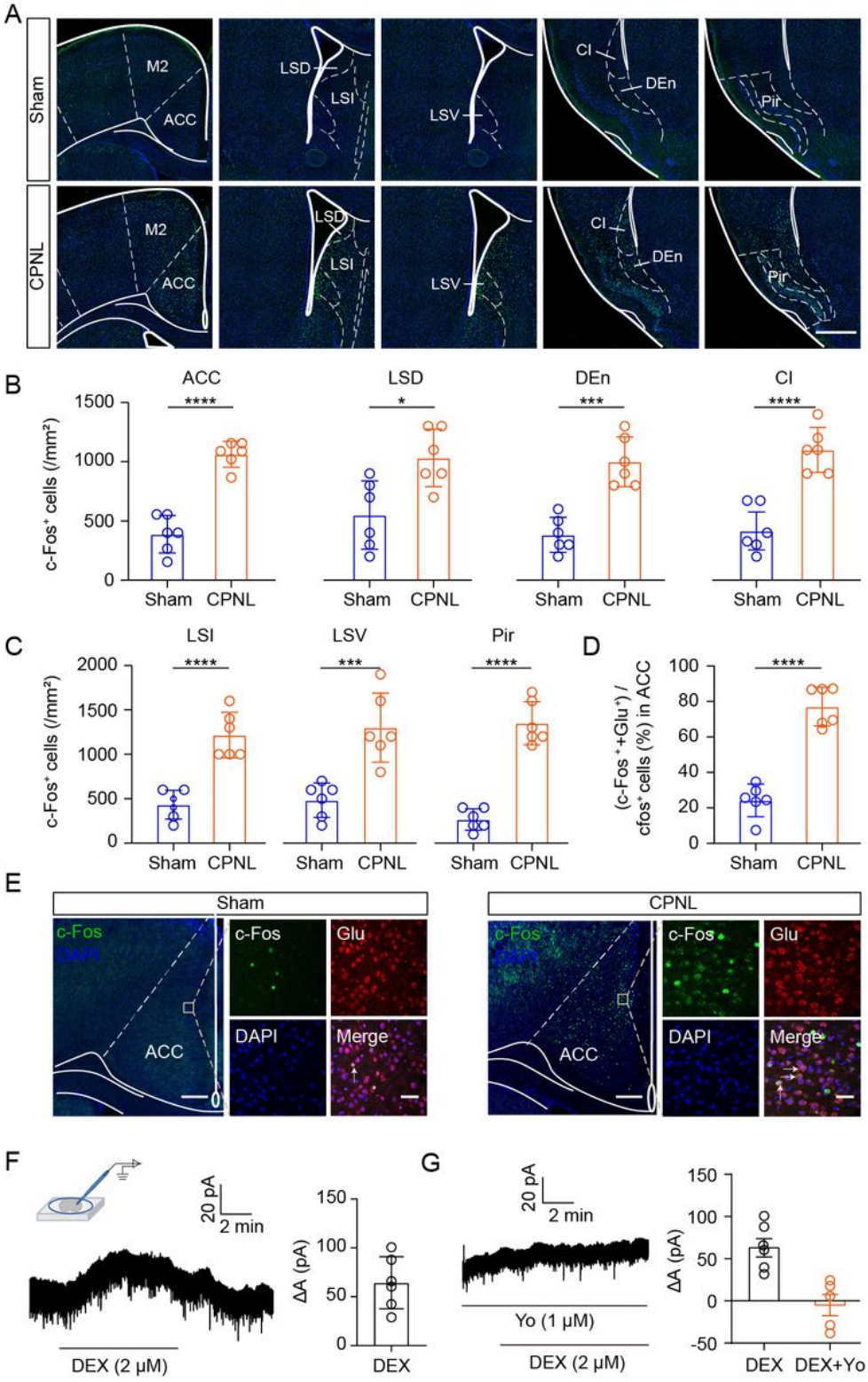

Figure 4

Glutamate neurons within the contralateral ACC are involved in the development of anxiety-like behaviors after CPNL.

(A) Typical images showing c-Fos in multiple brain regions in right brain slices on postsurgical day 10. Scale bars: 10000 μm. (B and C) The statistical data of c-Fos expression in the different brain regions (n =

6 mice per group, ACC: t10 = 8.61, $P < 0.001$, LSD: t10 = 3.145, $P = 0.010$, DEn: t10 = 5.895, $P < 0.001$, CI: t10 = 6.740, $P < 0.001$, LSI: t10 = 6.315, $P < 0.001$, LSV: t10 = 4.593, $P = 0.001$, Pir: t10 = 9.777, $P < 0.001$). (D and E) Statistical data (D) and representative images (E) showing c-Fos-labeled neurons colocalized with glutamate immunofluorescence within the right ACC at day 10 after CPNL. Scale bars: 200 μm (left) and 20 μm (right) (n = 6 mice per group, t10 = 9.053, $P < 0.0001$). (F) A representative trace of current and summarized data showing that GluACC neurons hyperpolarized in the presence of DEX (2 mM) and recovered during washout. (G) A representative trace of current and summarized data showing that yohimbine (1 mM) reversed the effect of DEX (2 mM) on GluACCneurons. Vhold = −60 mV. The period of drug application is indicated by the black line. The experiment was independently repeated in six neurons from 3 mice, and similar results were obtained. Compared with sham mice, $^{*}P < 0.05$, $^{**}P < 0.01$, $^{***}P < 0.001$, $^{****}P < 0.0001$. Two-tailed unpaired Student's t test for (B, C and D). ns, no significant difference; CPNL, common peroneal nerve ligation; ACC, anterior cingulate cortex; M2, secondary motor cortex; LSD, lateral septal nucleus, dorsal part; LSI, lateral septal nucleus, intermediate part; LSV, lateral septal nucleus, ventral part; CI, caudal interstitial nucleus of the medial longitudinal; Den, dorsal end piriform claustrum; Pir, piriform cortex.

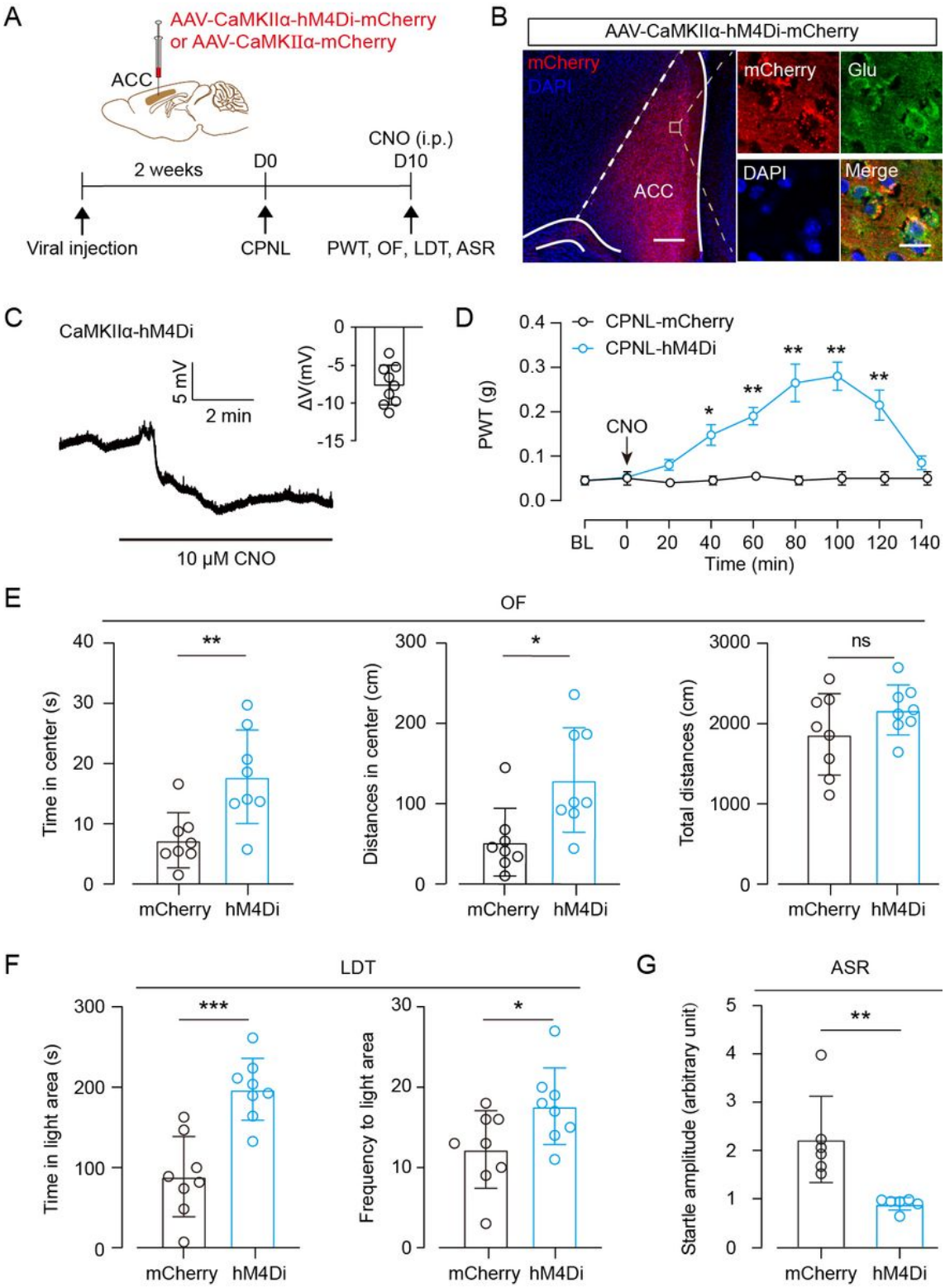

Figure 5

Inhibition of GluACCneuronal excitability alleviates pain-related and anxiety-like behaviors in CPNL mice.

(A) Schematic of virus injection and CNO administration. (B) Representative imaging of hM4Di virus expression in GluACC neurons. Scale bars: 200 μm (left) and 20 μm (right). (C) Representative trace (left) and summarized data (right) showing bath application of CNO (10 μM) hyperpolarizes GluACC neurons

(n = 9 neurons from 3 mice). (D) Changes in PWT after inhibition of GluACC neurons (n = 8 mice per group; time×group interaction, F (8, 112) = 12.45, $P < 0.001$). (E) Performance of CPNL mice treated with CNO in the OF test. (n = 8 mice per group; time in center, t14 =3.308, $P = 0.005$; distances in center, t14 = 2.832, $P = 0.013$; total distance, t14 = 1.449, $P = 0.1693$). (F) Performance of CPNL mice treated with CNO in the LDT test. (n = 8 mice per group; time in light area, t14 = 4.868, $P < 0.001$; frequency to light area, t14 = 2.237, $P = 0.042$). (G) Performance of CPNL mice treated with CNO in the ASR test (n = 6 mice per group; startle amplitude, t10 = 3.619, $P = 0.005$). Compared with mCherry-control mice, $* P < 0.05$, $** P < 0.01$, $*** P < 0.001$. Two-way repeated-measures (RM) ANOVA with Bonferroni post hoc analysis for (D); two-tailed unpaired Student's t test for (E, F and G). ANOVA, analysis of variance; ns, no significant difference; GluACC neurons, glutamatergic neurons in the anterior cingulate cortex; ACC, anterior cingulate cortex; CPNL, common peroneal nerve ligation; CNO, clozapine-N-oxide; PWT, paw withdrawal threshold; OFT, open field; LDT, light-dark transition; ASR, acoustic startle reflex.

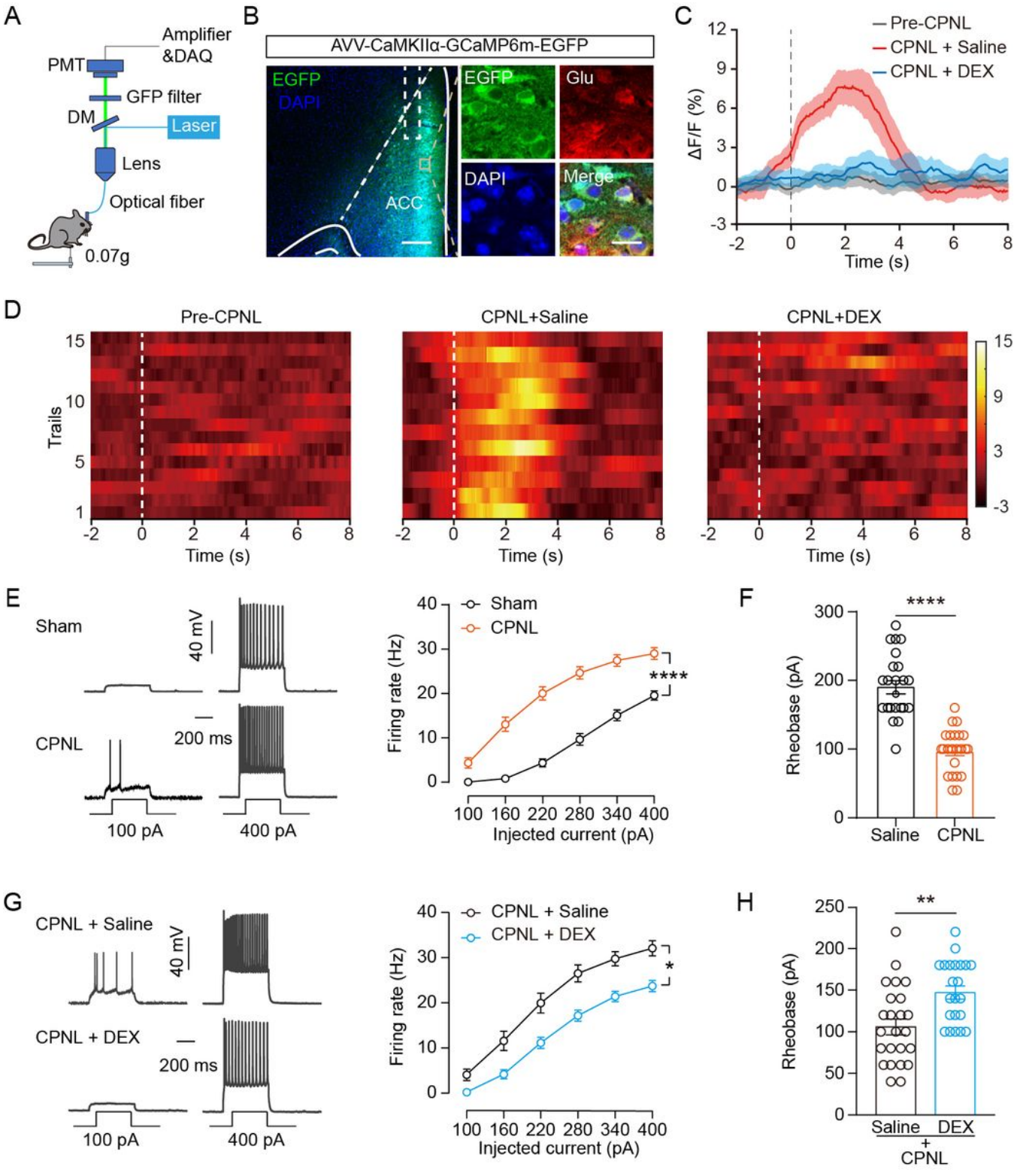

Figure 6

Increased GluACC neuronal excitability after CPNL can be inhibited by dexmedetomidine.

(A) Schematic of fiber photometry. DM: dichroic mirror; PMT: photomultiplier tube; DAQ: data acquisition. (B) Representative imaging of GCaMP6m viral expression in GluACCneurons. Scale bars: 200 μm (left) and 20 μm (right). (C-D) Data (C) and heatmaps (D) showing changes in calcium signals in saline- or

DEX-treated CPNL mice. The colored bar on the right indicates ΔF/F (%). (E) Representative traces (left) and summarized data (right) for action potential firing recorded from GluACC neurons in sham and CPNL mice. (n = 23 cells from 3 mice for each group. current×group interaction, F(5, 220) = 28.15, $P < 0.001$). (F) Summary of the rheobases from GluACCneurons in sham and CPNL mice. (n = 23 cells from 3 mice for each group. t44= 8.080, $P < 0.001$). (G) Representative traces (left) and summarized data (right) for action potential firing recorded from GluACC neurons in CPNL mice treated with saline or DEX. (n = 24 cells from 3 mice for the saline group, n = 22 cells from 3 mice for the DEX group. current×group interaction, F(5, 220) = 2.862, $P = 0.016$). (H) Summary of the rheobases from GluACC neurons in CPNL mice treated with saline or DEX. (n = 24 cells from 3 mice for the saline group, n = 22 cells from 3 mice for the DEX group. t44 = 3.312, $P = 0.002$). Compared with sham mice, $* P < 0.05$, $** P < 0.01$, $**** P < 0.0001$. Two-way repeated-measures (RM) ANOVA with Bonferroni post hoc analysis for (E and G); two-tailed unpaired Student's t test for (F and H). ANOVA, analysis of variance; ns, no significant difference. DEX, dexmedetomidine; GluACC neurons, glutamatergic neurons in the anterior cingulate cortex; ACC, anterior cingulate cortex; CPNL, common peroneal nerve ligation.

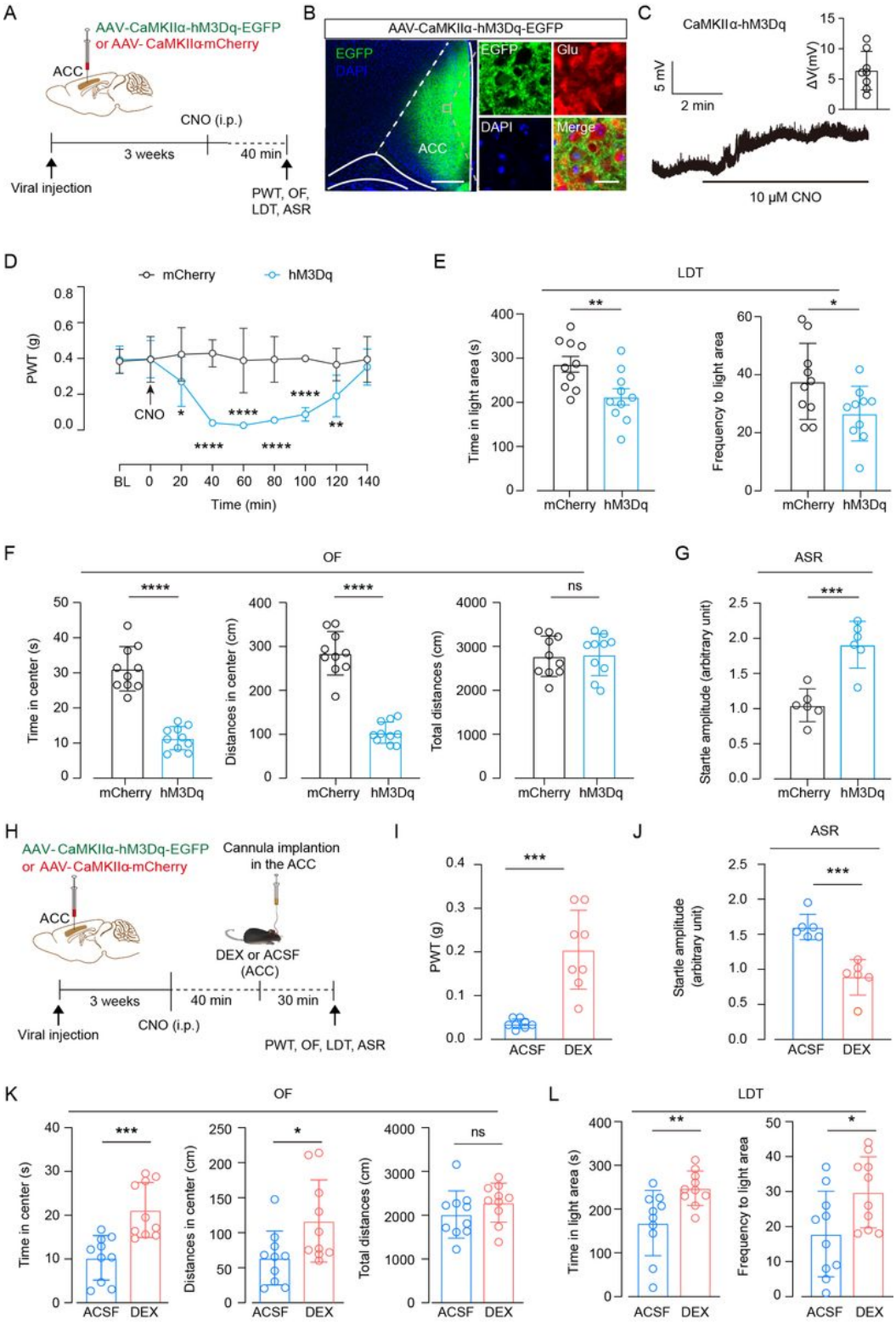

Figure 7

Increased GluACCneuronal excitability induced pain-related and anxiety-like behaviors in normal mice, which is rescued by intra-ACC dexmedetomidine.

(A) Schematic of virus injection. (B) Representative imaging of hM3Dq virus expression in GluACC neurons. Scale bars: 200 μm (left) and 20 μm (right). (C) Representative trace (left) and summarized data

(right) showing bath application of CNO (10 μM) depolarizes GluACC neurons (n = 8 neurons from 3 mice). (D) Changes in PWT after activation of GluACCneurons from CaMKIIα-hM3Dq mice. (n = 10 mice per group; time×group interaction, F (8, 120) = 11.69, $P < 0.001$). (E) Effects of chemogenetic activation of GluACCneurons from CaMKIIα-hM3Dq mice in the LDT test. (n = 10 mice per group; time in light area, t18 = 2.908, $P = 0.009$; frequency to light area, t18 = 2.174, $P = 0.043$). (F) Performance of CaMKIIα-hM3Dq mice treated with CNO in the OF test. (n = 10 mice per group; time in center, t18= 8.777,$P < 0.001$; distances in center, t18 = 10.31, $P < 0.001$; total distance, t18 = 0.1803, $P = 0.859$). (G) Performance of CPNL mice treated with CNO in the ASR test (n = 6 mice per group; startle amplitude, t10 = 5.207, $P < 0.001$). (H) Schematic of virus injection and timeline of experiment. Dexmedetomidine (2 μM) was injected into the ACC 40 min after CNO intraperitoneal administration. (I) Changes in PWT from CaMKIIα-hM3Dq mice treated with CNO and DEX. (n = 8 mice per group; t14 = 5.276, $P < 0.001$). (J) Performance from CaMKIIα-hM3Dq mice treated with CNO and DEX in the ASR test (n = 6 mice per group; startle amplitude, t10 = 5.645, $P < 0.001$). (K) Performance of CaMKIIα-hM3Dq mice treated with CNO and DEX in the OF test. (n = 10 mice per group; time in center, t18 =4.278, $P < 0.001$; distances in center, t18 = 2.373, $P = 0.029$; total distance, t18 = 1.214, $P = 0.240$). (L) Effects from CaMKIIα-hM3Dq mice treated with CNO and DEX in the LDT test. (n = 10 mice per group; time in light area, t18 = 2.983, $P = 0.008$; frequency to light area, t18 = 2.371, $P = 0.029$). Compared with CNO+ACSF mice, $* P < 0.05$, $** P < 0.01$, $*** P < 0.001$, $**** P < 0.0001$. Two-way repeated-measures (RM) ANOVA with Bonferroni post hoc analysis for (D); two-tailed unpaired Student's t test for (E, F, G, I, J, K and L). ANOVA, analysis of variance; ns, no significant difference; GluACC neurons, glutamatergic neurons in the ACC; ACC, anterior cingulate cortex; CPNL, common peroneal nerve ligation; DEX, dexmedetomidine; CNO, clozapine-N-oxide; ACSF, artificial cerebrospinal fluid; PWT, paw withdrawal threshold; OFT, open field; LDT, light-dark transition; ASR, acoustic startle reflex.